

Nonstationarity and $1/f$ noise characteristics in heart rate

BERNDT PILGRAM^{1,2} AND DANIEL T. KAPLAN³

¹Centre for Nonlinear Dynamics, McGill University, Montreal, Quebec, Canada H3G 1Y6;

²Institut für Mathematik, Universität Graz, A-8010 Graz, Austria; and ³Department of Mathematics and Computer Science, Macalester College, Saint Paul, Minnesota 55105

Pilgram, Berndt, and Daniel T. Kaplan. Nonstationarity and $1/f$ noise characteristics in heart rate. *Am. J. Physiol. Regulatory Integrative Comp. Physiol.* 45: R1–R9, 1999.—The power spectrum of human heart rate (HR) measured over 24 h exhibits “power-law” $1/f^\alpha$ -type spectral behavior with $\alpha \approx 1$. We investigate possible nonstationarity in time of the exponent α using maximum likelihood estimation, which allows relatively short data segments to be used. Examination of 24-h HR records from ambulatory normal and congestive heart failure (CHF) subjects indicates that the power-law structure of HR is nonstationary. In addition, α varies with time scale and is different for normal ($\alpha \approx 1$) and CHF ($\alpha \approx 1.5$) subjects. Simulations suggest that a possible mechanism underlying the observed power-law spectrum may be a switching between values of α near zero (white noise) and near two (Brownian motion). This mechanism generates power-law forms quantitatively similar to CHF subjects when the switching occurs very rapidly and similar to normal subjects when the switching is less rapid.

power law; control; self-similarity; model; surrogate data

IT HAS BEEN NOTED by numerous investigators (10, 12, 16, 20) that the variance of human heart rate (HR) or R-R intervals tends to increase when examined on longer and longer time scales. When examined using spectral analysis, this increase has the form of a “power law” where the squared amplitude of the Fourier transform at frequency f is proportional to $1/f^\alpha$. Generically, this form is called “one-over- f noise” and indeed it is found empirically that in heart rate $\alpha \approx 1$, as first reported by Kobayashi and Musha (10).

Figure 1A shows a 2-h segment of a 24-h R-R interval time series. Figure 1B depicts the power spectrum $P(f)$ for the entire 24-h record. One can divide the power spectrum into two main parts. At frequencies above ~ 0.02 Hz (or, equivalently, time scales < 50 s) the HR does not have $1/f$ structure and in fact shows the two well-known broad peaks: one at the frequency of respiration and one at a time scale of 10 s. At frequencies below ~ 0.02 Hz the power spectrum is well approximated by a straight line of slope $\alpha \approx -1$. Because the power spectrum is being plotted on log-log axes, this straight line corresponds to a power-law relationship $P(f) \sim 1/f^\alpha$.

Although $1/f^\alpha$ noise is observed in a wide diversity of physical, technological, and biological systems, e.g., river flows (4), traffic densities (9), and loudness fluctuations in speech and music (22), there is currently no

general explanation for its ubiquity and no generally satisfactory framework for its modeling in specific instances. In cardiac physiology, where there are numerous interacting control systems and adapting mechanisms with a wide range of time scales (3), it is of interest to know why a single exponent α should describe the relationship between fluctuations on time scales from 1 min to several hours.

We are interested here in two questions: Is the exponent α constant, independent of frequency (for $f < 0.2$ Hz)? Is the exponent α constant over time?

METHODS

The fundamental method we employ for assessing possible changes in α with time involves dividing a 24-h R-R interval time series into short segments, computing an estimate $\hat{\alpha}$ in each segment and checking whether $\hat{\alpha}$ is statistically significantly different from one segment to another. However, we confront the trade-off between bias and variance: to track rapid changes in α we need to use short segments, but to get reliable estimates $\hat{\alpha}$ we want segments to be long. Although this trade-off is unavoidable, we optimize our estimates $\hat{\alpha}$ by using an efficient maximum likelihood estimator (MLE) of α . This MLE has been found to provide estimates that are superior to linear regression on the logarithmic power spectrum or to Hurst-exponent type estimators (13, 1).

Time-Rescaling Analysis

When one divides a long time series into segments, one is implicitly setting the lowest frequency that can be considered in each segment. If we wish to include frequency f in the analysis, our segments must have length at least $1/f$ s. For instance, for frequency scales down to 0.0002 Hz, data segments must be $> 5,000$ s.

The interval T_s between samples sets the highest frequency that can be considered ($1/2T_s$). In studying the $1/f^\alpha$ structure of R-R intervals, we would like to be able explicitly to set both the upper and lower frequency bounds. When using a fast Fourier transform (FFT) estimator this is straightforward: explicitly set the frequency window over which linear regression is performed and ignore other frequencies. The MLE technique does not directly permit this, but we can still impose frequency bounds via the segment length and by setting the sampling interval T_s . The method that we have developed, which we term time rescaling analysis (TRA), consists of the following steps: 1) interpolate the raw R-R interval sequence into evenly spaced samples with $T_s = 0.5$ s; 2) pick a lower and upper frequency of interest (f_{lower} and f_{upper}); 3) anti-alias filter and resample the time series with a sampling interval of $T_s = 1/2 f_{\text{upper}}$; 4) divide the resampled time series into segments of length (L) = $1/f_{\text{lower}}$ (in the work reported here, we make our segments $L = 256$ points, giving $f_{\text{lower}} = f_{\text{upper}}/128 = f_{\text{upper}}/2^7$; thus we cover 7 octaves of the frequency scale). 5) For each segment, use MLE to compute the estimate $\hat{\alpha}$.

The costs of publication of this article were defrayed in part by the payment of page charges. The article must therefore be hereby marked “advertisement” in accordance with 18 U.S.C. Section 1734 solely to indicate this fact.

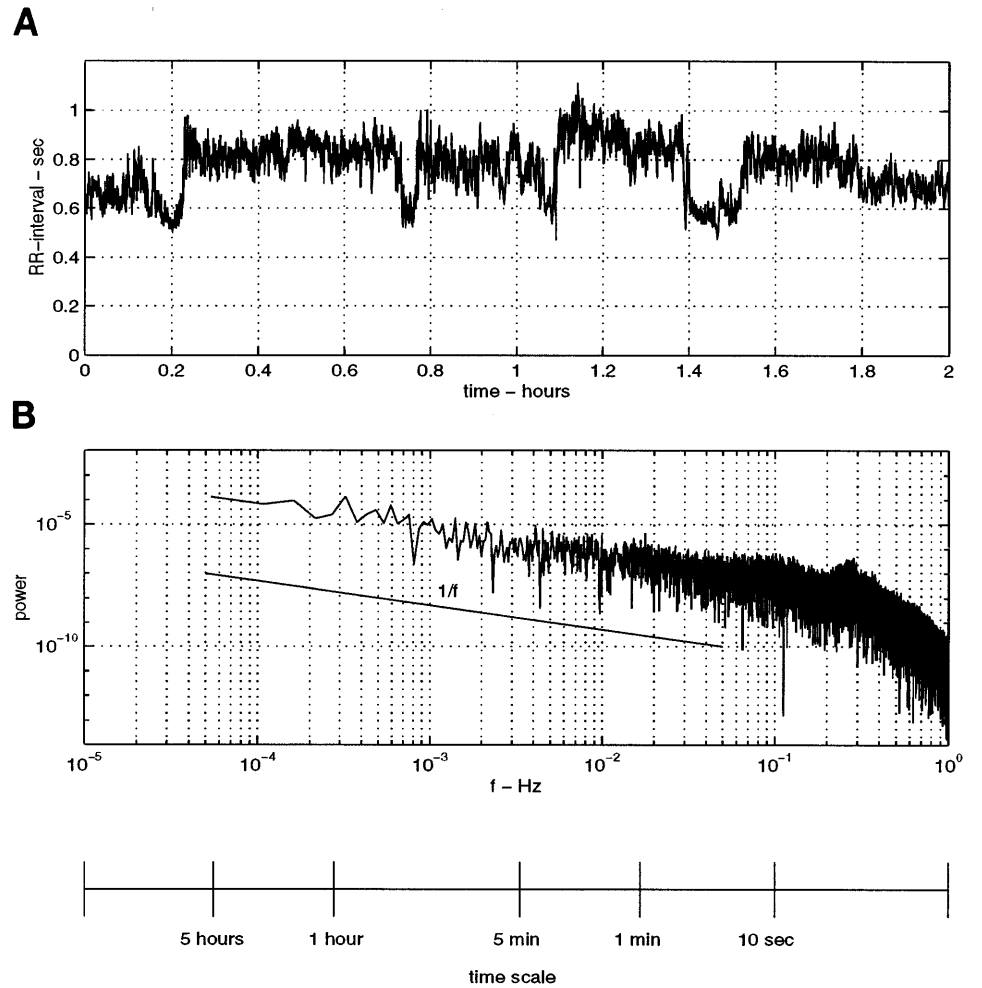


Fig. 1. *A*: 2-h segment of a 24-h R-R interval time series. *B*: power spectrum of the entire 24-h record, estimated using a fast Fourier transform (FFT)

At this point, we have a time series of $\hat{\alpha}$: one estimate for each segment. This time series can be examined directly to detect changes in α over time, as in Figs. 2A and 3A.

To investigate how α depends on the frequency f_{lower} , we repeat *steps 1–5* for several different values of f_{lower} , as seen in Figs. 2B and 3B, where the results are formatted in terms of $T_s = 1/2T_s$.

Assessing Statistical Significance

Figure 2 shows the results of applying the TRA technique to a synthetic signal whose power spectrum (estimated from the FFT) is a perfect power law with $\alpha = 1$. It can be seen (Fig. 2A) that the estimates $\hat{\alpha}$ vary somewhat from segment to segment. Because the synthetic signal is constructed to be stationary, we know that this is sampling variability and results from the fact that each segment is a sample from the perfect power-law signal.

In considering whether nonstationarity in α is responsible for segment-to-segment variation in $\hat{\alpha}$, we need to take into account sampling variability. One way to do this is to use synthetic data of the sort generated in Fig. 2 that has a perfect power-law structure. This approach was used in previous work studying the sampling distribution of the MLE estimator (13). However, it has not yet been established that R-R interval data is indeed perfect power-law data. We have therefore used a more general technique for generating synthetic data: the method of surrogate data (7, 8, 19).

Surrogate data are obtained in the following way: 1) take the Fourier transform of the original time series; 2) random-

ize the phases at each frequency to be uniformly distributed in $[0, 2\pi]$; 3) take the inverse Fourier transform.

Because the amplitude of the Fourier transform remains unchanged in *step 2*, the power spectra of the surrogate data and the original data are identical. Different realizations of surrogate data, all with the same power spectrum, can be generated by using different random phases in *step 2*.

Surrogate data exhibit the following important characteristics. 1) By construction, surrogate data are equivalent to linear filtering of stationary Gaussian white noise. 2) The process that generates surrogate data is stationary, i.e., the coefficients of the filter process remain constant as do the properties of the Gaussian white noise.

Thus surrogate data stem from a linear and stationary process. We note that although surrogate data have the same linear correlations as the original data, any nonlinear correlations in the original data do not appear in the surrogate data. Insofar as nonlinear correlations exist in R-R interval data [a controversial issue that is the subject of current research (6, 7, 14, 17)], the surrogate data will be qualitatively different from the R-R interval data. However, although nonlinearities might possibly be important in the generation of $1/f^\alpha$ noise, estimates of α based on spectral analysis or the MLE method used here will be insensitive to the nonlinear correlations in the data. Therefore we claim that surrogate data provide an appropriate statistical technique for estimating the sampling distribution of the MLE estimator. However, without a specific model of how some nonlinearity underlies $1/f^\alpha$ noise, we

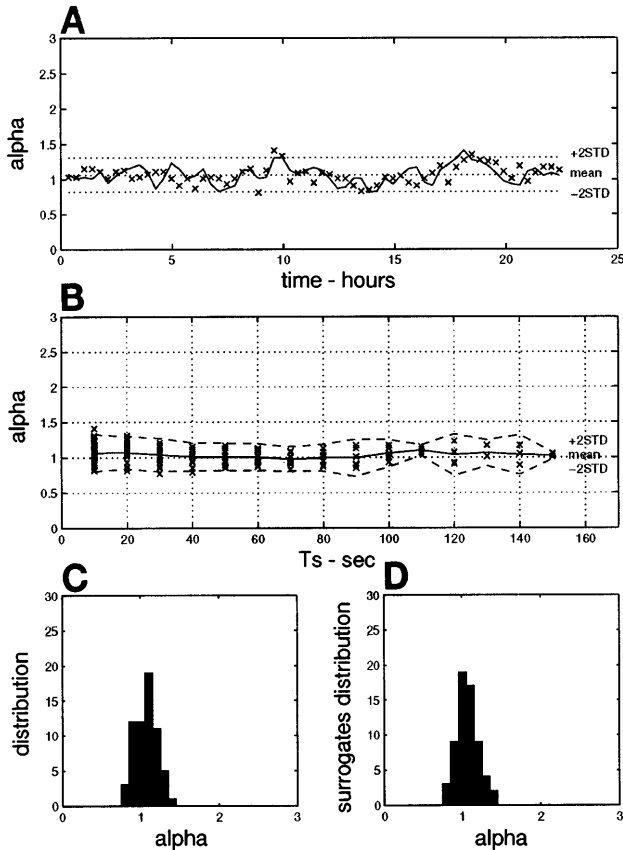


Fig. 2. Analysis of the simulated perfect $1/f$ process. *A*: estimated exponent $\hat{\alpha}$ vs. time for $T_s = 10$ s for simulated data (solid line) showing mean ± 2 SD (dotted lines) of all surrogate sets and 1 set of surrogates (x marks). *B*: Time rescaling analysis (TRA) showing exponents $\hat{\alpha}$ vs. sampling time T_s with mean ± 2 SD at each T_s . *C*: histogram for $\hat{\alpha}$ shown in *A*. *D*: histogram for $\hat{\alpha}$ from surrogates shown in *A*.

do not know how to construct an empirical test of the validity of this claim.

Using surrogate data, we can estimate the sampling distribution for $\hat{\alpha}$ for a stationary process with the same power spectrum as the 24-h R-R interval data. We use three approaches to investigating whether the distribution from surrogate data differs from that of the original R-R interval data; we term this the stationarity-in-time analysis.

The first approach is to graphically display the histograms of the segment-by-segment estimates $\hat{\alpha}$ for the R-R interval data and a surrogate data set. If the R-R interval data have a nonstationary α , the histogram should be broader for the R-R interval data than for the surrogate data. In addition, we plot out a time series of $\hat{\alpha}$ versus time for both the R-R-interval data and one realization of surrogate data.

The second approach is to quantify the width of the distribution of $\hat{\alpha}$ using the interquartile range and compare the width of the estimates $\hat{\alpha}$ for the R-R interval to the estimates for 10 different realizations of surrogate data using a two-sided t -test.

A third approach is to characterize general differences in the distribution using the Kolmogorov-Smirnov (K-S) test (15, 21). The K-S measure d is defined as the maximum value of the absolute difference between two cumulative distribution functions. For each R-R interval time series we obtain a set of estimates $\hat{\alpha}$. Ten realizations of surrogate data are used, producing 10 sets of $\hat{\alpha}$ from stationary processes. First, we

compare the data estimates to each of the 10 surrogate estimates using the K-S statistic and obtain 10 measures $D = (d_1, d_2, \dots, d_{10})$. Then, we compare each of the surrogate estimates to each other and obtain $10 \times 9/2 = 45$ measures $D_s = (ds_1, ds_2, \dots, ds_{45})$. Finally, we perform Student's t -test to determine whether the two samples D and D_s could have the same mean.

We note that surrogate data were developed originally (19) to detect nonlinearity in possibly chaotic data. This use involves employing a statistic that is sensitive to nonlinear structure. Here, we use a statistic $\hat{\alpha}$ that is based on the autocorrelation function and hence models the signal as linear. Because of this, differences between the surrogates and the test data do not point directly to nonlinearity of the test data. Instead, they reflect other violations of the null hypothesis associated with surrogate data, in particular the stationarity of surrogate data.

Illustration of the Techniques Using Synthetic Data

To illustrate the stationarity-in-time and TRA analyses, we consider three synthetic time series: 1) a “perfect” stationary $1/f$ time series where α is constant in time and the same at all frequencies; 2) a time series where α changes in time but is the same at all frequencies at each time; 3) a time series where α is different for different frequency bands, but is constant in time.

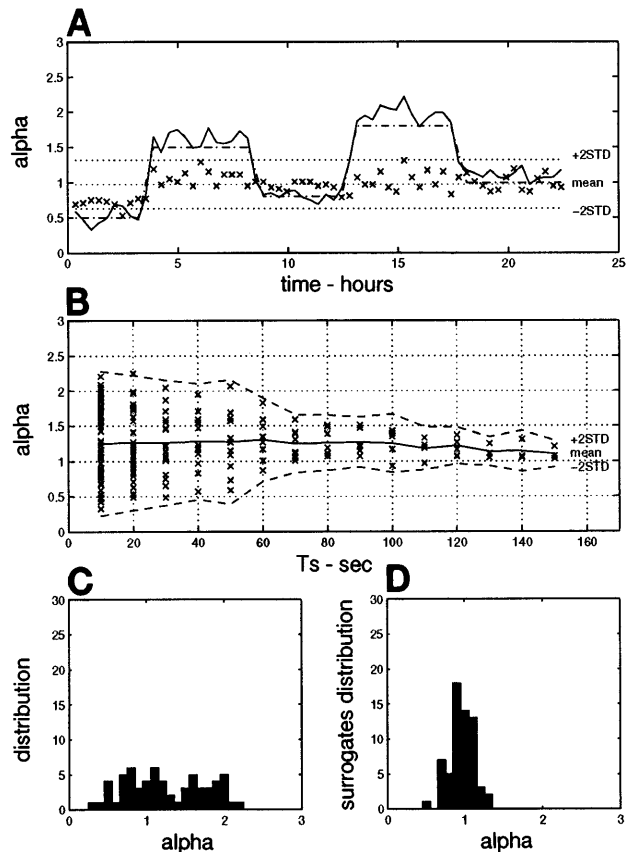


Fig. 3. Analysis of the simulated time-varying $1/f^\alpha$ process. *A*: estimated exponent $\hat{\alpha}$ vs. time for $T_s = 10$ s for simulated data (solid line) showing mean ± 2 SD (dotted lines) of all surrogate sets and 1 set of surrogates (x marks). Dashed line indicates exponent α used for generation of simulated data as a function of time. *B*: TRA showing exponents $\hat{\alpha}$ versus sampling time T_s with mean ± 2 SD at each T_s . *C*: histogram for $\hat{\alpha}$ shown in *A*. *D*: histogram for $\hat{\alpha}$ from surrogates shown in *A*.

α *Stationary in time, independent of frequency.* A perfect $1/f$ time series of length 65,536 sample points was generated using a spectral synthesis method, and then a subsample of length 8,192 was used as our test data as in Ref. 13. A length of 8,192 is roughly the same as the 24-h R-R interval time series when sampled every 10 s.

For the stationarity-in-time analysis, the time series was sampled every 10 s (that is, the 8,192 point time series was used directly) and overlapping segments of length $L = 256$ points were used. For the TRA analysis, the time series was sampled at $T_s = 10$ s, 20 s, . . . 150 s and divided into segments of length 256 points.

Figure 2 and Table 1 show the results. Sampling fluctuations are visible in Fig. 2A, but these are not qualitatively different than the surrogate data (shown as x in Fig. 2A). The histograms showing the spread of $\hat{\alpha}$ are essentially identical; the interquartile range (IQR) of the distribution of $\hat{\alpha}$ from the $1/f$ time series (IQR_d) and the IQR of the distribution of $\hat{\alpha}$ from surrogates (IQR_s) are roughly the same. The K-S computations similarly show that the distribution of $\hat{\alpha}$ for the $1/f$ time series is not significantly different than that of the surrogates, which is underlined by a significance level $P < 0.40$. Thus there is no indication of nonstationarity in time here, as would be expected for this type of synthetic signal.

In Fig. 2B, the estimate $\hat{\alpha}$ is plotted for each sampling time T_s for each segment. For fast sampling times (e.g., 10 s) there are many segments in the whole time series and consequently many estimates $\hat{\alpha}$ (plotted as x). For slow sampling times (e.g., 100 s), there are fewer segments and thus fewer estimates for $\hat{\alpha}$. Note that at a sampling time of 100 s, the time scales comprehended by one estimation range up to 7.1 h. There is no evidence for a time-scale dependence of α , as expected for this type of signal.

α *Changes in time, independent of frequency.* The ability of MLE to track nonstationarity was tested by estimating the exponent α of test data simulating time-varying behavior of exponent α . The data set was generated by concatenating time series, 256 data points long, with time-varying α in the range 0.5–1.8. As seen in Fig. 3A, the estimates $\hat{\alpha}$ (solid line) track closely the α used in the simulation (dashed line). The surrogates show no such pattern. The histogram of $\hat{\alpha}$ is much broader for the nonstationary data than for the surrogate data (which has more or less the same width as in the stationary case illustrated in Fig. 2).

Figure 3B depicts all the estimates $\hat{\alpha}$ versus sampling time T_s . Here $\hat{\alpha}$ is approximately constant over a wide range of time scales, although there is no single α in this data set. This suggests that a nonperfect power-law process may appear to have a $\hat{\alpha}$ that is independent of frequency. But note that the range of $\hat{\alpha}$ in Fig. 3B is much wider than in Fig. 2B, reflecting the nonstationarity of the signal in Fig. 3. This is also underlined by the results from the statistical analysis given in Table 1, $P < 0.0001$.

Table 1. *Synthetic time series*

| Case No. | IQR _d | IQR _s | STD _{IQR} | t | Significance, % |
|----------|------------------|------------------|--------------------|-------|-----------------|
| 1 | 0.17 | 0.14 | 0.02 | -0.85 | 39.72 |
| 2 | 0.90 | 0.22 | 0.03 | 48.53 | 0.00 |
| 3 | 0.14 | 0.15 | 0.02 | 1.14 | 26.05 |

Interquartile ranges (IQR) and results of the t -test using Kolmogorov-Smirnov (K-S) statistic describing differences between distributions of data estimates $\hat{\alpha}$ and the surrogate estimates: IQR_d of the data estimates, mean IQR_s, and standard deviation STD_{IQR} of the corresponding surrogate sets, Student's value t from K-S measures D and D_s of estimates and probability significance in % of an observed value of t for D and D_s from synthetic time series.

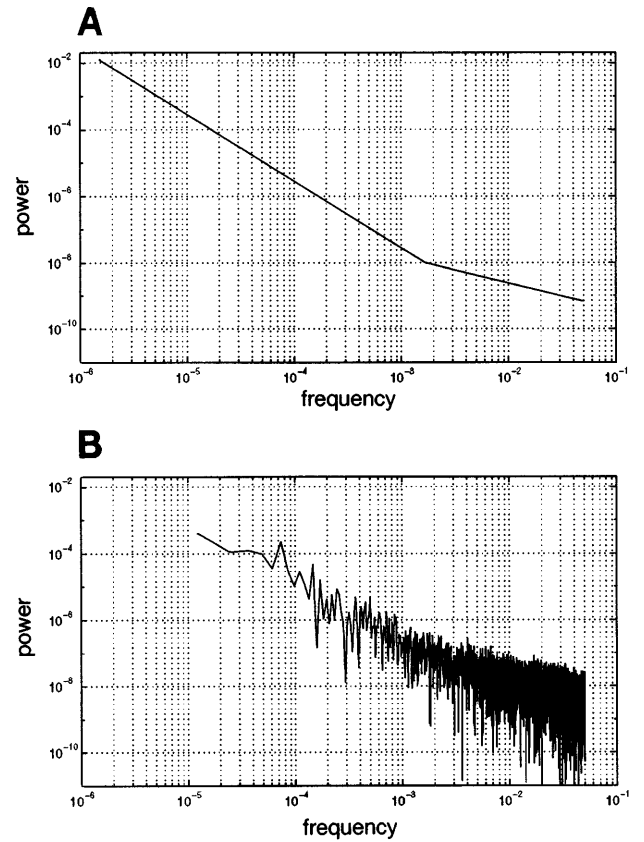


Fig. 4. A: Power spectrum of a perfect frequency-varying $1/f^\alpha$ process with $\alpha = 0.8$ for time scales smaller than 10 min, i.e. frequencies higher than $f = 1.7 \cdot 10^{-3}$, $\alpha = 2$ for larger time scales, and of length $n = 2^{16}$ (64 K). B: power spectrum of a segment of length $n = 2^{13}$ (8 K) of the signal in A.

α *Stationary in time, but changes with frequency.* The ability of TRA to discern variations in α at different frequencies is illustrated by application to a time series with frequency-varying exponent α . A time series of length $2^{16} = 65,536$ was synthesized. The power spectrum (Fig. 4A) shows that $\alpha = 2$ for $f < 0.0017$ and $\alpha = 0.8$ for $f \geq 0.0017$. For the analysis, a segment of length 8,192 was extracted. The power spectrum of this segment (Fig. 4B) closely mimics power spectra seen in studies of HR.

The stationarity-in-time analysis (Fig. 5A, C, and D; Table 1) gives no indication of nonstationarity, as is to be expected for this stationary time series. The TRA analysis (Fig. 5B) shows a clear drift in $\hat{\alpha}$ with time scale.

The power spectrum in Fig. 4A gives a clearer indication of MLE of the structure of α as a function of frequency f than does TRA (Fig. 5B). However, this is misleading. Only those data in Fig. 4B were used in the TRA analysis, and realistic data of any length will always have the sampling fluctuations seen in Fig. 4B. The precise straight-line form in Fig. 4A does not incorporate the sampling variability that must be present in any experimentally collected data set. We encourage the reader to perform the following experiment. Without reference to Fig. 4A, locate the frequency at which the bend in Fig. 4B occurs. Compare your estimate to the frequency clearly indicated in 4A. We find that an error by a factor of two is typical.

Quantitative estimate of α from the power spectrum requires that linear regression be performed. Figure 6 shows the result of such a regression on the power spectrum in Fig.

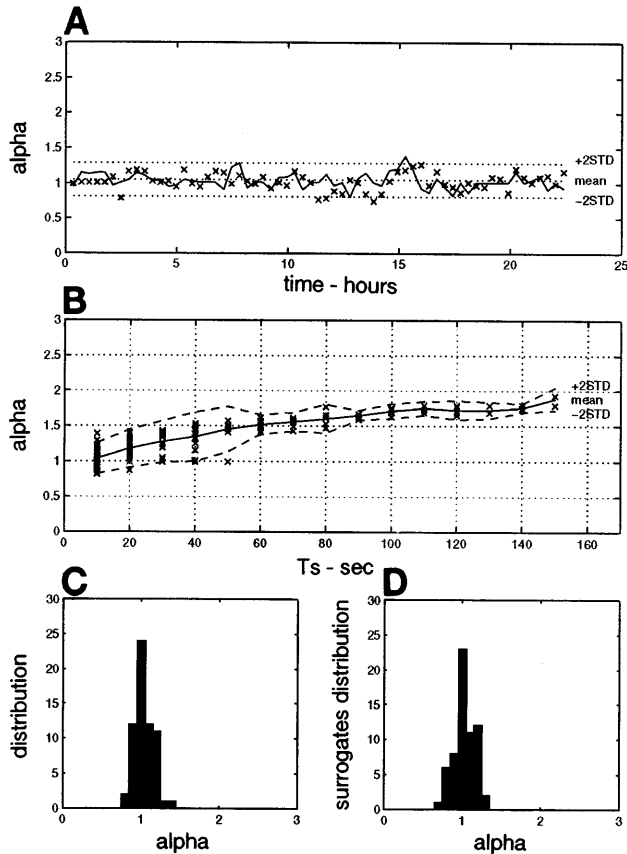


Fig. 5. Analysis of the simulated frequency-varying $1/f^\alpha$ process shown in Fig. 4. *A*: estimated exponent $\hat{\alpha}$ vs. time for $T_s = 10$ s for simulated data (solid line) showing mean ± 2 SD (dotted lines) of all surrogate sets and 1 set of surrogates (x marks). *B*: TRA showing exponents $\hat{\alpha}$ vs. sampling time T_s with mean ± 2 SD at each T_s . *C*: histogram for $\hat{\alpha}$ shown in *A*. *D*: histogram for $\hat{\alpha}$ from surrogates shown in *A*.

4*B*. Linear regression was performed over a window from f_{lower} to f_{upper} , and $\hat{\alpha}$ was estimated as the slope of the line as a function of f_{upper} . To facilitate comparison with TRA, we have formatted the results as a function of $T_s = 1/f_{\text{upper}}$. Figure 6 shows regressions done with frequency windows of seven (same as used in TRA), six, and five octaves. The shorter windows do not make clearer the sharp transition from $\alpha = 2$ to $\alpha = 0.8$.

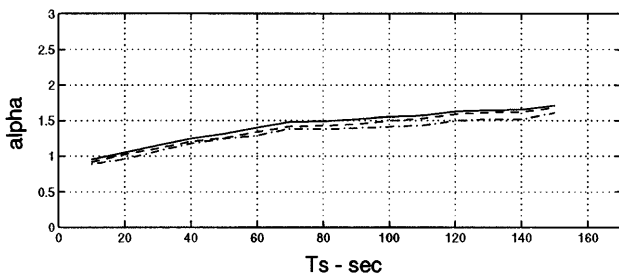


Fig. 6. Exponents $\hat{\alpha}$ from linear regression on a moving window of the power spectrum in Fig. 4*B* vs. frequency f_{upper} of the window (formatted in terms of sampling time T_s). Three different lengths of the regression window are shown, covering a frequency range of 7 (solid line), 6 (dashed line), and 5 octaves (dash-dotted line) data points.

ANALYSIS OF HEART RATE

We applied the stationarity-in-time and TRA analysis to 20 recordings of R-R intervals over 24 h from which abnormal beats had been deleted. These time series were provided to us by C. K. Peng and A. L. Goldberger (see Ref. 12). There were 9 healthy subjects and 11 congestive heart failure (CHF) patients.

Figures 7 and 8 show the stationarity-in-time and TRA analysis for a representative normal subject and a representative CHF patient. In both cases, nonstationarity in α is suggested by the broad histograms of $\hat{\alpha}$ for the R-R interval data compared with the surrogate data. The CHF patient shows clear sustained deviations in $\hat{\alpha}$ from the mean value that last for several hours.

The TRA analysis shows that for the CHF subject $\hat{\alpha}$ increases from ≈ 1 at T_s near 20 s to ≈ 1.5 at T_s near 100 s. This pattern is sustained in almost all of the records. Figure 9 shows the TRA analysis for all 20 records. The CHF patients typically show a higher $\hat{\alpha}$ than the normal patients at large time scales (corresponding to low frequencies).

The stationarity-in-time analysis is presented for all of the subjects in Fig. 10 and Table 2. In almost all subjects, the IQR of the distribution of $\hat{\alpha}$ is roughly

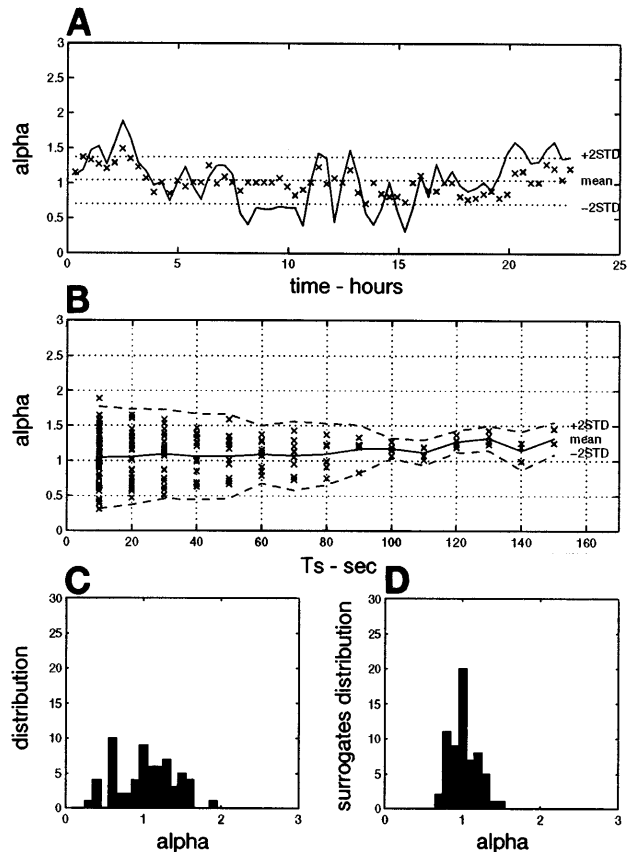


Fig. 7. Results of the analysis of case no. 16,786, a normal subject. *A*: estimated exponent $\hat{\alpha}$ vs. time for $T_s = 10$ s for R-R interval data (solid line) showing mean ± 2 SD (dotted lines) of all surrogate sets and 1 set of surrogates (x marks). *B*: TRA showing exponents $\hat{\alpha}$ vs. sampling time T_s with mean ± 2 SD at each T_s . *C*: histogram for $\hat{\alpha}$ shown in *A*. *D*: histogram for $\hat{\alpha}$ from surrogates shown in *A*.

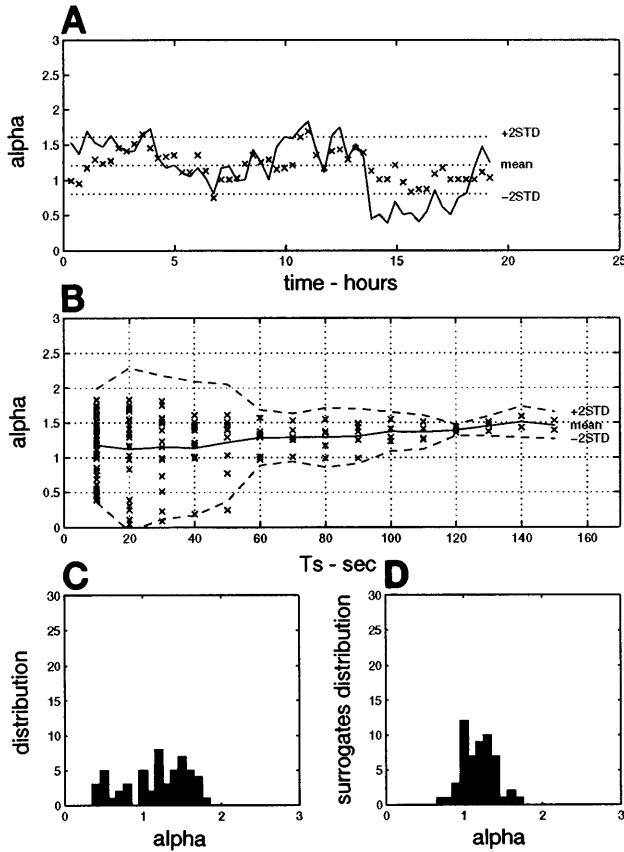


Fig. 8. Results of the analysis of case no. 9,706, a congestive heart failure (CHF) subject. *A*: estimated exponent $\hat{\alpha}$ vs. time for $T_s = 10$ s for R-R interval data (solid line) showing mean ± 2 SD (dotted lines) of all surrogate sets and 1 set of surrogates (x marks). *B*: TRA showing exponents $\hat{\alpha}$ vs. sampling time T_s with mean ± 2 SD at each T_s . *C*: histogram for $\hat{\alpha}$ shown in *A*. *D*: histogram for $\hat{\alpha}$ from surrogates shown in *A*.

twice as large in the R-R interval data compared with the width expected purely due to sampling variability (as indicated by surrogate data). The K-S computations similarly show that the distribution of $\hat{\alpha}$ for the R-R interval data is different than that of the surrogates and point to this difference being statistically significant at a level $P < 0.01$ in all except CHF subject 9,778.

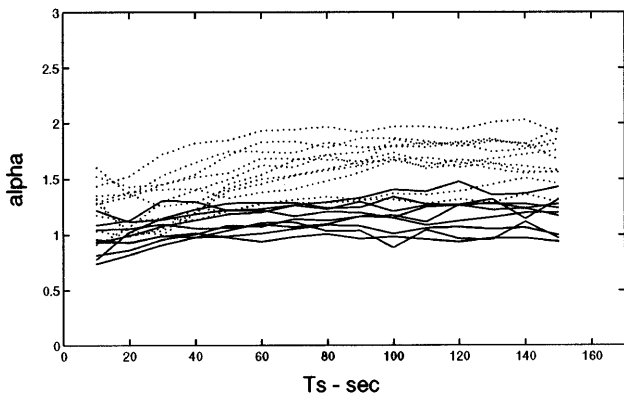


Fig. 9. Estimated exponents $\hat{\alpha}$ vs. sampling time T_s for 24-h R-R interval data from 11 CHF patients (dotted lines) and 9 normal subjects (solid lines). Mean $\hat{\alpha}$ for each subject at each T_s is plotted.

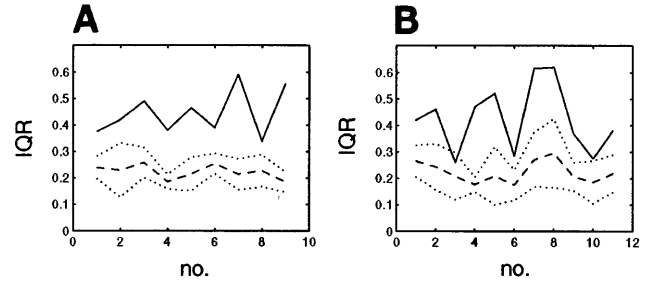


Fig. 10. Interquartile range (IQR) of $\hat{\alpha}$ vs. patient index no. for sampling time $T_s = 10$ s. *A*: IQR of $\hat{\alpha}$ from normals (solid line) and mean IQR ± 2 SD of all corresponding surrogate sets (dashed and dotted lines). *B*: IQR of $\hat{\alpha}$ from CHF patients (solid line) and mean IQR ± 2 SD of all corresponding surrogate sets (dashed and dotted lines).

DISCUSSION

R-R interval time series show in almost all cases “mixed” process behavior, i.e., exponent α exhibits time and frequency dependence. Similar results were also found by Meesmann et al. (11), who showed that in the HR of young healthy subjects, periods of $1/f$ noise had intermittent subperiods of white noise during the night. Ichimaru and Katayama (5) suggest that the exponent α may be different for each sleep stage. Di Rienzo et al. (2) found that $\hat{\alpha}$ measured via power-spectral regression varied with frequency f .

One possibility suggested by Fig. 3 is that nonstationarity and the observed $1/f^{\hat{\alpha}}$ pattern in HR are related. In that figure, $\hat{\alpha} \approx 1$ at large T_s , although α is not constant. For instance, at $T_s = 140$ s, estimates are being made using segments that span 10 h, during which time α is

Table 2. Results of *t*-test using K-S statistic describing differences between distributions of data estimates α and surrogate estimates for sampling time $T_s = 10$ s

| Index | Case No. | <i>t</i> | Significance, % |
|--|----------|----------|-----------------|
| <i>Normal subjects</i> | | | |
| 1 | 16,265 | 9.69 | 0.00 |
| 2 | 16,273 | 7.01 | 0.00 |
| 3 | 16,420 | 11.53 | 0.00 |
| 4 | 16,483 | 3.38 | 0.14 |
| 5 | 16,539 | 14.53 | 0.00 |
| 6 | 16,773 | 11.88 | 0.00 |
| 7 | 16,786 | 21.14 | 0.00 |
| 8 | 17,052 | 2.90 | 0.54 |
| 9 | 17,453 | 12.51 | 0.00 |
| <i>Congestive heart failure subjects</i> | | | |
| 1 | 8,519 | 10.53 | 0.00 |
| 2 | 8,679 | 6.85 | 0.00 |
| 3 | 9,049 | 6.43 | 0.00 |
| 4 | 9,377 | 15.06 | 0.00 |
| 5 | 9,435 | 9.90 | 0.00 |
| 6 | 9,643 | 7.53 | 0.00 |
| 7 | 9,674 | 23.47 | 0.00 |
| 8 | 9,706 | 6.73 | 0.00 |
| 9 | 9,723 | 15.12 | 0.00 |
| 10 | 9,778 | 1.90 | 6.22 |
| 11 | 9,837 | 7.05 | 0.00 |

Student's value *t* from K-S measures D and D_s of estimates and probability significance in % of an observed value of *t* for D and D_s from data of normal and congestive heart failure subjects.

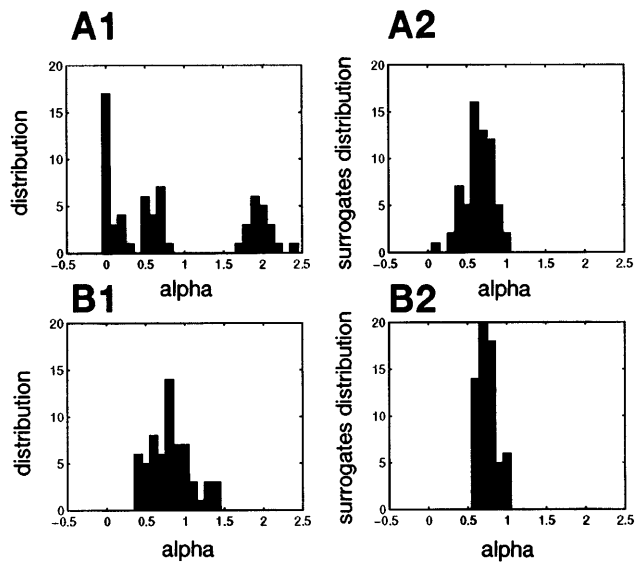


Fig. 11. Histograms $\hat{\alpha}$ from the model nonstationary process (see DISCUSSION). *A1*: results from data generated by concatenation of model segments 256 data points long. *A2*: results from its surrogates. *B1*: results from data generated by concatenation of model segments 32 data points long. *B2*: results from its surrogates.

varying substantially, yet $\hat{\alpha}$ at these long segment lengths does not vary much from segment to segment.

Although there is no general theoretical explanation for systems with $\alpha = 1$, there are simple theoretical models for $\alpha = 0$ (white noise) and $\alpha = 2$ (Brownian motion, the cumulative sum of white noise). Is it possible that a system that switches between white noise and Brownian motion might produce $\hat{\alpha} = 1$?

From our stationarity-in-time analysis of R-R interval data, there is no reason to suspect that the periods of white noise or Brownian motion might last for as long as one analysis segment (2,560 s). If this were the case, we would expect to see values of $\hat{\alpha}$ near 0 or 2, but we do not. Instead, we hypothesize that the switching might occur much faster, over say one-quarter or one-half of the analysis segment (320 s or 640 s).

In terms of control systems, Brownian motion corresponds to control being turned off, whereas white noise variability indicates that control is on: the system may be knocked off its set point by an outside disturbance, but quickly returns to it, only to be knocked off again. But why should HR control be turned off?

HR is one of several effector variables involved in regulating the cardiovascular system. By “effector vari-

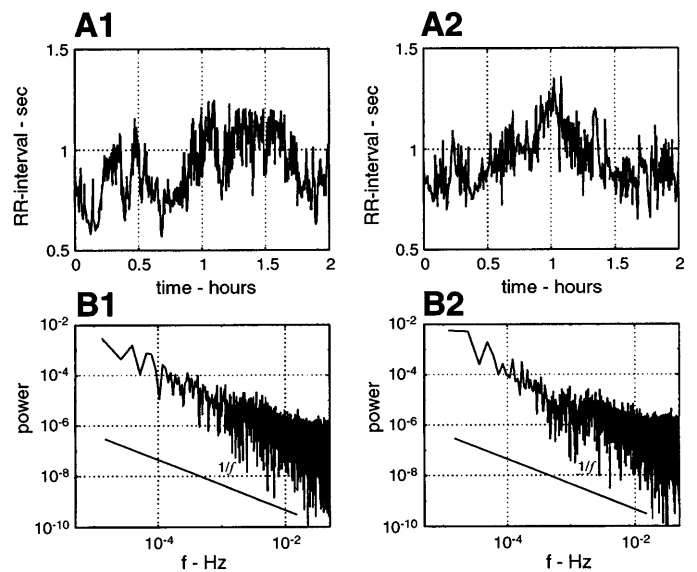


Fig. 13. *A1*: a 2-h segment of an R-R interval time series sampled at $T_s = 10$ s. *A2*: 2-h segment from the nonstationary model of α . *B1*: power spectrum of a 24-h R-R interval time series showing $1/f$ -like spectral behavior. *B2*: power spectrum of 24-h simulated time series showing $1/f$ -like spectral behavior.

able” we mean a feature of the system that is used to bring a regulated quantity to the appropriate level or range of levels. Other effector variables are peripheral resistance, blood volume, and vascular compliance. Examples of regulated quantities are blood pressure and blood gas levels that are directly sensed or cardiac output measured indirectly via blood gas levels and blood pressure. Note that HR is generally considered not to be a regulated quantity; it is a means to an end rather than an end in itself. Although there are baroreceptors and chemoreceptors to measure blood pressure and blood gas levels, there is no analogous receptor for HR. This suggests that HR might be allowed to drift (Brownian motion). However, drifts in HR might be punctuated by periods of resetting when control systems attempt to use HR as an effector variable and therefore HR is locked in to the appropriate value for the quantity that is being regulated.

In addition, control systems acting on very long time scales (e.g., the renal blood-volume control system) might indirectly affect HR via other feedback loops. This could cause slow, long-term drifts in HR. All told, HR might be seen as episodes of Brownian motion

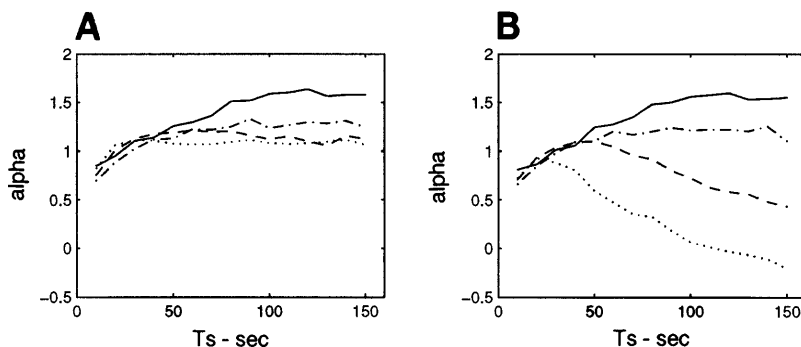


Fig. 12. TRA analysis on the model nonstationary process. $\hat{\alpha}$ vs. sampling time T_s for 4 nonstationary test data sets generated by concatenating white and Brownian motion segments with different segment lengths, 256 (solid line), 128 (dash-dotted line), 64 (dashed line), and 32 (dotted line) data points. *A*: TRA results from time series with local random trends added. *B*: TRA results from time series without local random trends.

interrupted by episodes of white noise for short time scales, all on a background of slow trends.

To model this hypothesized structure for HR, we concatenated short segments of Gaussian white noise and Brownian motion. For each segment, we made a random choice between white noise and Brownian motion. As a background, we added to each segment a linear trend with a random direction for each segment. These trends were matched at their endpoints. Note that none of these three processes individually produce $1/f$ noise: white noise has $\alpha = 0$, Brownian motion has $\alpha = 2$, and the piecewise linear trends have $\alpha = 2$ for low frequencies and $\alpha = 0$ for high frequencies.

Figure 11 shows the histograms of the estimated exponents $\hat{\alpha}$ (sampling time $T_s = 10$ s) for data produced by our model process where model segments 256 (Fig. 11A) and 32 data points long were concatenated (Fig. 11B). For a model segment length of 256 data points, the estimates $\hat{\alpha}$ are able to resolve the time series into $1/f^0$ and $1/f^2$ segments, expressed by two main peaks at $\alpha = 0$ and $\alpha = 2$ in the histogram. For model segments of length 32, $\hat{\alpha}$ is not able to resolve the time-varying character of exponent α . The histograms of $\hat{\alpha}$ from surrogate data are substantially narrower than for the model data, providing the same kind of evidence for nonstationarity seen in the R-R interval data.

Figure 12A, which depicts the TRA analysis of $\hat{\alpha}$ vs. T_s shows a pattern similar to that seen in the R-R interval data. We point out the similarity of the short model segment (32 points) TRA to that found in normal subjects, and the long model segment (256 points) TRA to that found in CHF patients.

Figure 12B shows the effect of deleting the local linear trends part of the model. For the short model segment ("healthy") data, there is a loss of verisimilitude.

Visual comparison (Fig. 13) of a randomly selected segment of R-R interval data from a normal subject and a synthetic signal from the nonstationary segments-with-trend model of α suggests that this simple model produces realistic time series with realistic power spectra.

This simple model of the $1/f^{\hat{\alpha}}$ structure of HR suggests that the power-law structure of HR may be nonstationary over fairly short intervals, similar to the 5-min segments commonly used in short-term HR variability analysis (18). It also points to a possible difference between cardiovascular control in normal and CHF subjects.

In addition, the stationarity-in-time analysis raises the question of whether it is possible to obtain more information about the $1/f^{\hat{\alpha}}$ behavior of HR data by analyzing longer time series. The answer might be no. The range of exponents encountered indicates that the observed $1/f^{\hat{\alpha}}$ pattern might be a property of the interaction of the estimators with nonstationarity in the exponent α , as we have seen in the simulations.

Perspectives

Our statistical analysis of 24-h HR records indicates that the $1/f^{\hat{\alpha}}$ structure in HR fluctuates in time and that α varies with time scale. Analysis of 24-h records as a whole shows α is ~ 1 , but analysis of short segments (~ 1 h) shows that α fluctuates significantly. When looked at another way, concatenating many 1-h segments with widely varying α produces a 24-h signal with $\alpha \approx 1$.

We speculatively carry this process to an extreme: using computer simulations we show that by concatenating very short segments with $\alpha = 0$ or $\alpha = 2$ one produces 1-h segments where α is close to 1 but varies significantly on either side of it and 24-h patterns with α quite close to 1. We cannot confirm this rapid-switching model by direct measurement of α on very short segments: the statistical methods have too high a variance on the short segments and we would need to use even shorter segments to find out when the hypothetical switching occurs.

It may be possible to assess the rapid-switching model by measurements other than α . For instance, the amplitudes of the well-known 10-s and respiratory HR spectral peaks may vary as cardiac control switches from an $\alpha = 0$ to an $\alpha = 2$ pattern. At this point in the research, we see the value of the model as a way of supporting and organizing the hypothesis that the 24-h $1/f$ structure may be an epiphenomenon and is the statistical result of a conceptually much different process.

We thank C. K. Peng and A. Goldberger for providing us with the CHF and normal HR data used in this paper.

This study was partially supported by a "Kurt-Gödel-Fellowship" of the Austrian Ministry for Science and Research, by a fellowship from the Österreichische Forschungsgesellschaft, and by grants from the Natural Sciences and Engineering Research Council of Canada, the Fonds de la recherche en santé du Québec, and the Fonds pour la formation de chercheurs et l'aide à la recherche.

Address for reprint requests: D. T. Kaplan, Dept. of Mathematics and Computer Science, Macalester College, 1600 Grand Ave., St. Paul, MN 55105.

Received 8 April 1998; accepted in final form 14 September 1998.

REFERENCES

1. **Bassingthwaight, J. B., and G. M. Raymond.** Evaluating rescaled range analysis for time series. *Ann. Biomed. Eng.* 22: 432–444, 1994.
2. **Di Rienzo, M., G. Parati, A. Pedotti, and P. Castiglioni.** $1/f$ Modeling of blood pressure and heart rate spectra. In: *Frontiers of Blood Pressure and Heart Rate Analysis* edited by M. Di Rienzo, G. Mancia, G. Parati, A. Pedotti, and A. Zanchetti. Amsterdam: IOS, 1997.
3. **Guyton, A. C., T. G. Coleman, and H. J. Granger.** Circulation: overall regulation. *Ann. Rev. Physiol.* 34: 13–46, 1972.
4. **Hosking, J. R. M.** Modeling persistence in hydrological time series using fractional differencing. *Water Resources Res.* 5: 321–340, 1984.
5. **Ichimaru, Y., and S. Katayama.** Central nervous system and heart rate variability. In: *Noise in Physical Systems and 1/f Fluctuations*, edited by T. Musha, S. Sato, and Y. Yamamoto. Tokyo, Ohmsha: 1991, p 691–694.
6. **Kanters, J. K., N.-H. Holstein-Rathlou, and E. Agner.** Lack of evidence for low-dimensional chaos in heart rate variability. *J. Cardiovasc. Electrophysiol.* 5: 591–601, 1994.

7. **Kaplan, D. T.** Nonlinearity and nonstationarity: the use of surrogate data in interpreting fluctuations. In: *Frontiers of Blood Pressure and Heart Rate Analysis*, edited by M. Di Rienzo, G. Mancia, G. Parati, A. Pedotti, and A. Zanchetti. Amsterdam: IOS, 1997.
8. **Kaplan, D. T., and L. Glass.** *Understanding Nonlinear Dynamics*. New York: Springer Verlag, 1995.
9. **Keshner, M. S.** $1/f$ Noise. *Proc. IEEE* 70: 212–218, 1982.
10. **Kobayashi, M., and R. Musha.** $1/f$ Fluctuation of heartbeat period. *IEEE Trans. Biomed. Engin.* 29: 456–457, 1982.
11. **Meesmann, M., F. Grüneis, P. Flachenecker, and K.-D. Knifki.** A new method for analysis of heart rate variability: counting statistics of $1/f$ fluctuations. *Biol. Cybern.* 68: 299–306, 1993.
12. **Peng, C. K., S. Havlin, H. E. Stanley, and A. L. Goldberger.** Quantification of scaling exponents and crossover phenomena in nonstationary heartbeat time series. *Chaos* 5: 82–87, 1995.
13. **Pilgram, B., and D. T. Kaplan.** A comparison of estimators for $1/f$ noise. *Physica D* 114: 108–122, 1998.
14. **Poon, C.-S., and C. K. Merrill.** Decrease of cardiac chaos in congestive heart failure. *Nature* 389: 492–495, 1997.
15. **Press, W. H., S. A. Teukolsky, W. T. Vetterling, and B. P. Flannery.** *Numerical Recipes in C: The Art of Scientific Computing* (2nd ed.). Cambridge, UK: Cambridge University Press, 1992.
16. **Saul, J. P., P. Albrecht, R. D. Berger, and R. J. Cohen.** Analysis of long term heart rate variability: methods, $1/f$ scaling and implications. In: *Computers in Cardiology*. Silver Spring, MD: IEEE Computer Society, p. 419–422, 1987.
17. **Sugihara, G., W. Allan, D. Sobel, and K. D. Allan.** Nonlinear control of heart rate variability in human infants. *Proc. Natl. Acad. Sci. USA* 93: 2608–2613, 1996.
18. **Task Force of the European Society of Cardiology and NASPE.** Heart rate variability: standards of measurement, physiological interpretation, and clinical use. *Circulation* 93: 1043–1065, 1996.
19. **Theiler, J., S. Eubank, A. Longtin, B. Galdrikian, and J. D. Farmer.** Testing for nonlinearity in time series: the method of surrogate data. *Physica D* 58: 77–94, 1992.
20. **Turcott, R. G., and M. C. Teich.** Fractal character of the electrocardiogram: distinguishing heart-failure and normal patients. *Ann. Biomed. Engin.* 24: 269–293, 1996.
21. **Von Mises, R.** *Mathematical Theory of Probability and Statistics*. New York: Academic, 1964.
22. **Voss, R. F., and J. Clarke.** $1/f$ noise in music and speech. *Nature* 258: 317–318, 1975.

